Available online at www.sciencedirect.com
SCIENCE DIRECT®
Applied Catalysis A: General 254 (2003) 239–249
APPLIED CATALYSIS A: GENERAL
www.elsevier.com/locate/apcata

Mesoporous H-AlMCM-48: highly efficient solid acid catalyst

S.E. Dapurkar [a], P. Selvam [a,b,*]

[a] *Department of Chemistry, Indian Institute of Technology-Bombay, Powai, Mumbai 400076, India*
[b] *Department of Materials Chemistry, Tohoku University, Aoba-yama 07, Sendai 980-8579, Japan*

Received 18 March 2003; received in revised form 8 April 2003; accepted 14 April 2003

Abstract

Mesoporous cubic Na-AlMCM-48 molecular sieve catalyst with a Si/Al (molar) ratio of 60 was synthesized hydrothermally and characterized by various analytical and spectroscopic techniques. ^{27}Al MAS-NMR results indicate that the presence of aluminum in tetrahedral framework (Brönsted acid site) in both as-synthesized and calcined samples. However, in the case of the latter, a small amount of aluminum was found to be in octahedral coordination. This observation is well supported by NH_3-TPD studies over protonated catalyst (H-AlMCM-48), where desorption profile at higher temperature shows features characteristic of Lewis acid sites. Further, these studies also indicate that the presence of high concentration of moderate-to-strong Brönsted acid sites at lower temperature, which are more suitable for the *para*-selective *tertiary*-butylation reaction of phenol. Hence, in the present investigation, the reaction was carried out H-AlMCM-48, which however showed much higher activity as compared to the hexagonal H-AlMCM-41. In addition, it was also found that the former does not get deactivated owing to three-dimensional pore system while the latter is susceptible to deactivation on account of one-dimensional pore system.
© 2003 Elsevier B.V. All rights reserved.

Keywords: Mesoporous; AlMCM-48; AlMCM-41; Solid acid catalyst; *tert*-Butyl phenol

1. Introduction

The discovery of thermally stable silicate and aluminosilicate mesoporous molecular sieves having one-dimensional hexagonal MCM-41 and three-dimensional cubic MCM-48 structure [1] has attracted significantly research interest and opened up new opportunities in many areas, in particular heterogeneous catalysis [2–6]. Further the unique surface properties of these materials, which combine high surface areas with large pore diameters and pore volumes, render themselves as versatile catalysts over microporous analogues. It is well known that both framework and extra-framework aluminum in molecular sieves generates both Brönsted and Lewis acid sites and thus function as solid acid catalysts for several acid-catalyzed reactions [3–7]. In this regard, the protonated mesoporous AlMCM-41 and AlMCM-48 (designated as H-AlMCM-41 and H-AlMCM-48, respectively) show promise for such purpose. It is, however, noteworthy here that despite the successful development of H-AlMCM-41 catalysts [8–25], only very little is known about H-AlMCM-48 (the sodium form of these cataand its characteristics such as the acidic strength, catalytic properties, etc. [15,26–29]. One of the main reasons being the difficulty encountered in the preparation of good quality samples owing to a narrower homogeneity region of the phase [30]. On the other hand, the three-dimensional pore opening of H-AlMCM-48 is promising due to resistant to

* Corresponding author. Tel.: +91-22-2576-7155; fax: +91-22-2572-3480.
E-mail address: selvam@chem.iitb.ac.in (P. Selvam).

0926-860X/$ – see front matter © 2003 Elsevier B.V. All rights reserved.
doi:10.1016/S0926-860X(03)00486-1

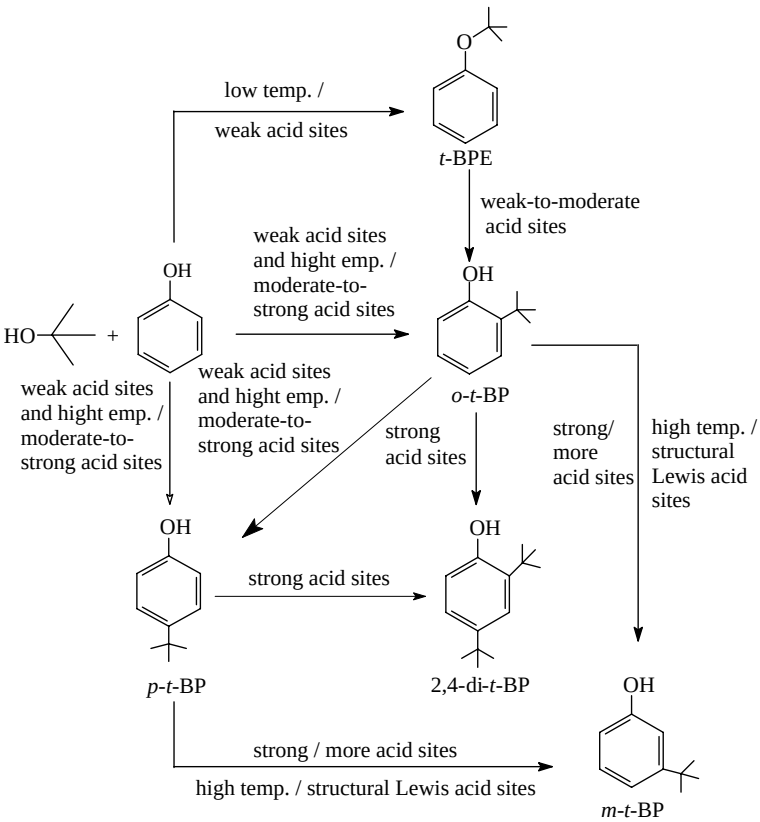

Scheme 1. Effect of experimental conditions and acidic sites on the *t*-butylation of phenol.

pore blocking as well as it entails more agitated flow, which increases the number of interactions between reactants and catalytic sites than the one-dimensional opening of H-AlMCM-41 [15,29,31–34], thus the former exhibits much higher activity than the latter. Hence, in this study attention has been focused on the potential application of mesoporous H-AlMCM-48 molecular sieves for the *tertiary*-butylation of phenol reaction, as the products, viz. *para-tert*-butyl phenol (*p-t*-BP) and 2,4-di-*tert*-butyl phenol (2,4-di-*t*-BP), are industrially important as they are widely used in the manufacture of phenolic resins, antioxidants and polymerization inhibitors [35].

Numerous studies on the production of these alkyl-substituted phenols over various heterogeneous solid acid catalysts have been reported in literature [23,36–47]. However, as shown in Scheme 1, the catalytic activity and selectivity of *t*-butyl phenol products, in general, has been found to depend on the acidic characteristics and reaction conditions as well as on the framework structure of the catalysts [23,36–47]. For example, weak acidic catalysts such as AlPO-11, AlPO-31, and AlPO-41 [38] produce *p-t*-BP, where as partially exchanged (Na^+ or K^+) zeolite-Y (weak acid catalyst) leads to oxygen-alkylated product (*tert*-butyl phenyl ether; *t*-BPE) [39]. However, strong acidic catalysts, e.g. zeolite-β and 13X-zeolite, produces *p-t*-BP [40,48] and/or carbon-alkylated product (*meta-tert*-butyl phenol; *m-t*-BP), which is formed by the secondary isomerization of initially formed *ortho-tert*-butyl phenol (*o-t*-BP) and *p-t*-BP [41]. On the other hand, moderate acidic catalysts like zeolite-Y [42], ZSM-12 [43], SAPO-11 [44], H-AlMCM-41 [23], H-FeMCM-41 [45] and H-GaMCM-41 [46] are found to favor the formation of *p*-isomer. Thus the selective formation of *p-t*-BP not only depends on the acidity but also on the experimental condition. In view of the importance of

tertiary-butylation of phenol as well as the promising characteristics of mesoporous H-AlMCM-48, in this study an attempt has been made to evaluate the catalytic activity of this catalyst for the *tertiary*-butylation of phenol reaction, and the results are presented herein.

2. Experimental

2.1. Starting materials

Aluminum sulfate ($Al_2(SO_4)_3{\cdot}18H_2O$; Aldrich; 98%), tetraethylorthosilicate (TEOS; Aldrich; 98%), fumed silica (SiO_2; Aldrich; 99.8%) and cetyltrimethylammonium bromide (CTAB, Aldrich; 99%) were used as sources for aluminum, silicon, and template, respectively. Sodium hydroxide (NaOH; Loba; 98%) and tetramethyl ammonium hydroxide (TMAOH; Aldrich; 25 wt.%) were used as alkali and organic base sources. Phenol (Merck; 99.5%), *tert*-butyl alcohol (*t*-BA; Thomas Baker; 99%) were used for (vapor phase) phenol alkylation reactions. Authentic samples of *o*-*t*-BP (Fluka; 99%), *meta*-*tert*-butyl phenol (Aldrich; 99%), *p*-*t*-BP (Fluka; 99%), and 2,4-di-*t*-BP (Fluka; 99%) were used for comparative analysis with the reaction products.

2.2. Synthesis of Na-AlMCM-48

The sodium-form of AlMCM-48 (referred as Na-AlMCM-48) with a Si/Al (molar) ratio of 60 was synthesized as per the procedure described else where [49] with a typical molar gel composition of: SiO_2:$0.25(Na_2O)_2$:$0.30(CTA)_2O$:$60H_2O$:$0.0083Al_2O_3$. Initially, 'Solution-A' was obtained by mixing NaOH and tetraethyl orthosilicate (TEOS) in distilled water under constant stirring for 10 min. 'Solution-B' was then prepared by dissolving CTAB in distilled water and was stirred for 20 min. Finally, a homogeneous transparent gel was obtained by mixing 'Solution-A' and 'Solution-B' under constant stirring for 25 min. In this resulting gel, aluminum source was added and stirred further for an hour for homogenization. The pH of final gel was 11.3 and kept for crystallization in Teflon-lined stainless steel autoclaves at 373 K for 72 h. The solid product obtained was washed repeatedly, filtered and dried at 353 K for 12 h. The as-synthesized material was calcined at 823 K for 2 h in N_2 followed by air for 6 h.

2.3. Preparation of H-AlMCM-48

The protonated form of the mesoporous aluminosilicate (H-AlMCM-48) was prepared from the calcined AlMCM-48 by an ion-exchange method as per the procedure given below. First, the ammonia-form of AlMCM-48 was obtained by repeated exchange of the sodium-form of AlMCM-48 with 1 M NH_4NO_3 at 353 K for 6 h. The H-AlMCM-48 was then obtained by deammoniation at 823 K for 6 h in air.

2.4. Synthesis of Na-AlMCM-41

The sodium-form of AlMCM-41 (referred as Na-AlMCM-41) with a Si/Al (molar) ratio of 60 was synthesized as per the procedure described else where [23] with a typical molar gel composition of: SiO_2:$0.13(Na_2O)_2$:$0.13(TMA)_2O$:$0.135(CTA)_2O$:$60H_2O$:$0.0083Al_2O_3$. Initially, 'Solution-A' was obtained by mixing a TMAOH and fumed silica in distilled water. 'Solution-B' was prepared by addition of CTAB and NaOH in distilled water. Both 'Solution-A' and 'Solution-B' were mixed together and aluminum source was added. It was stirred further for an hour for homogenization and kept for crystallization in Teflon-lined stainless steel autoclaves at 373 K for 24 h. The as-synthesized material was calcined at 823 K for 2 h in N_2 followed by air for 6 h. H-AlMCM-41 was prepared from the calcined Na-AlMCM-41 by an ion-exchange method.

2.5. Characterization

All the samples were systematically characterized by powder X-ray diffraction (XRD; Rigaku-miniflex), N_2 sorption isotherms (Sorptomatic-1990), transmission electron microscopy and electron diffraction (TEM and ED; Philips CM 200 operated at 200 kV), Fourier transform-infrared (FT-IR; Nicolet Impact 400) spectroscopy, ^{29}Si and ^{27}Al magic angle spinning-nuclear magnetic resonance (^{29}Si and ^{27}Al MAS-NMR; Varian VXR-300S), and inductively coupled plasma-atomic-emission spectroscopy (ICP-AES; Labtam Plasma 8440) techniques. The surface area was estimated using the Brunauer–Emmett–Teller

(BET) method and the pore size was calculated by Horvath–Kawazoe (H–K) approach. The pore volume was determined from the amount of N_2 adsorbed at $P/P_0 = 0.5$.

2.6. Temperature programmed desorption of ammonia

The acidic behavior of the H-AlMCM-48 catalyst was studied by temperature-programmed desorption of ammonia (NH_3-TPD) as per the procedure described elsewhere [23]. A 200 mg of H-AlMCM-48 was placed in a quartz reactor and was activated at 823 K in air for 6 h followed by 2 h in helium with a flow rate of 50 ml min^{-1}. The reactor was then cooled to 373 K and maintained for another hour under the same condition. Ammonia adsorption was carried out by passing the gas through the sample for 15–20 min at this temperature. Subsequently, it was purged with helium for an hour to remove the physisorbed ammonia. Finally, the desorption of ammonia was carried out by heating the reactor upto 873 K at 10 K min^{-1} using a temperature programmer (Eurotherm). The amount of ammonia desorbed was estimated with the aid of thermal conductivity detector (TCD) response factor for ammonia.

2.7. tertiary-Butylation of phenol

The *tertiary*-butylation of phenol was carried out using 750 mg of H-AlMCM-48 catalyst in a home-made fixed-bed flow reactor. Prior to the reaction, the catalyst was activated at 773 K in flowing air for 8 h followed by cooling to reaction temperature (448 K) under nitrogen atmosphere. After an hour, the reactant mixture, i.e. phenol and *t*-butyl alcohol (*t*-BA) with a desired (molar) ratio and weight hour space velocity (WHSV) was fed into the reactor using a liquid injection pump (Sigmamotor) with nitrogen as carrier gas. The gaseous products obtained were cooled and the condensed liquid products were collected at every 30 min interval.

2.8. Products analyses

The various products of the *tertiary*-butylation reaction, viz., *p*-*t*-BP, *o*-*t*-BP and 2,4-di-*t*-BP, were identified by gas chromatography (NUCON 5700) with SE-30 column. Further, *m*-*t*-BP was identified using AT1000 column. In addition, all these products were confirmed with the use of a combined gas chromatography–mass spectrometry (GC–MS; Hewlett G1800A) set-up fitted with HP-5 capillary column.

3. Results and discussion

Fig. 1 shows the XRD patterns of various AlMCM-48 samples. The diffraction patterns show all the major reflections, which are characteristic of a cubic mesoporous MCM-48 structure [1,2]. The calculated average unit cell parameter (a_0) for Na-AlMCM-48 was 88.0 Å, which is higher than the aluminum-free siliceous MCM-48 (80.2 Å). Similarly the unit cell parameter for Na-AlMCM-41 and siliceous MCM-41 were 48.10 and 44.77 Å respectively [23]. The increase in unit cell parameter could be attributed to the isomorphous substitution of trivalent aluminum for tetravalent silicon, as the crystal radius of the former (0.53 Å) is larger than the latter (0.40 Å) [50]. ICP-AES analyses of Na-AlMCM-48 indicate that the aluminum content (Si/Al = 61) in the catalyst remains nearly same as in the starting (gel) composition (Si/Al = 60) indicating almost

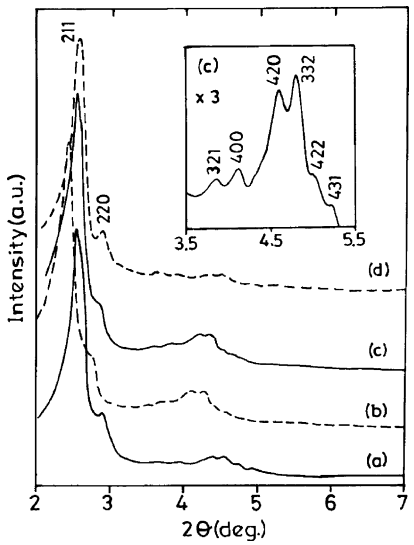

Fig. 1. XRD patterns of: (a) calcined Na-MCM-48, (b) calcined Na-AlMCM-48, (c) H-AlMCM-48 before reaction and (d) H-AlMCM-48 after reaction.

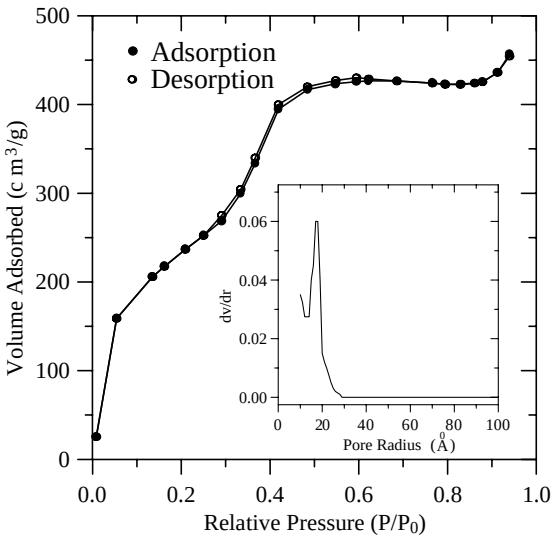

Fig. 2. N_2 adsorption–desorption isotherm of calcined Na-AlMCM-48 (inset shows pore size distribution).

a complete incorporation of aluminum in the matrix. Fig. 2 depicts the N_2 adsorption–desorption of calcined Na-AlMCM-48. The pore volume, surface area, and pore diameter deduced from the N_2 sorption measurement were $0.79\,ml\,g^{-1}$, $1018\,m^2\,g^{-1}$, and 34 Å, respectively. However, the pore volume, surface area, and pore diameter for Na-AlMCM-41 were $0.75\,ml\,g^{-1}$, $889\,m^2\,g^{-1}$, and 32 Å, respectively. TEM image of calcined Na-AlMCM-48 (Fig. 3a) indicates that the mesopores are arranged along the (1 1 0) cubic plane [51]. Further, an ED pattern confirms the good quality of the sample (Fig. 3b) [52].

Fig. 4 presents FT-IR spectra of various AlMCM-48 samples. The broad band in the region 3200–3800 cm^{-1} are assigned to surface hydroxyl groups. On the other hand, the bands at 2920 and 2848 cm^{-1} are characteristic of hydrocarbon moieties, which disappear upon calcinations indicating the removal of template molecules from the mesopores. The bands at 1230, 1080, and 460 cm^{-1}, are assigned to symmetric stretching and bending of ≡Si–O–Si≡ vibration while the weak bands at ∼960 cm^{-1} are attributed to defect sites (≡Si–OH) [33,53]. Since the $Si–O^-$ and $Al–O^-$ stretching bands appear nearly in the same region (800–1100 cm^{-1}) and hence they cannot be clearly distinguished. Further, it can also be noticed from Fig. 4 that that there is no appreciable change in spectral features before and after reaction (see Fig. 4c and d) thus indicating the intactness of structure.

Fig. 5 shows the ^{29}Si MAS-NMR spectra of as-synthesized and calcined Na-AlMCM-48. The spectrum of the former gives two main signals centered at −109.6 ppm, assigned to Q_4 site ($Si(OSi)_4$), and −100.6 ppm, assigned to Q_3 site ($Si(SiO)_3(OH)$), with a weak shoulder at −91.0 ppm attributed to Q_2 site

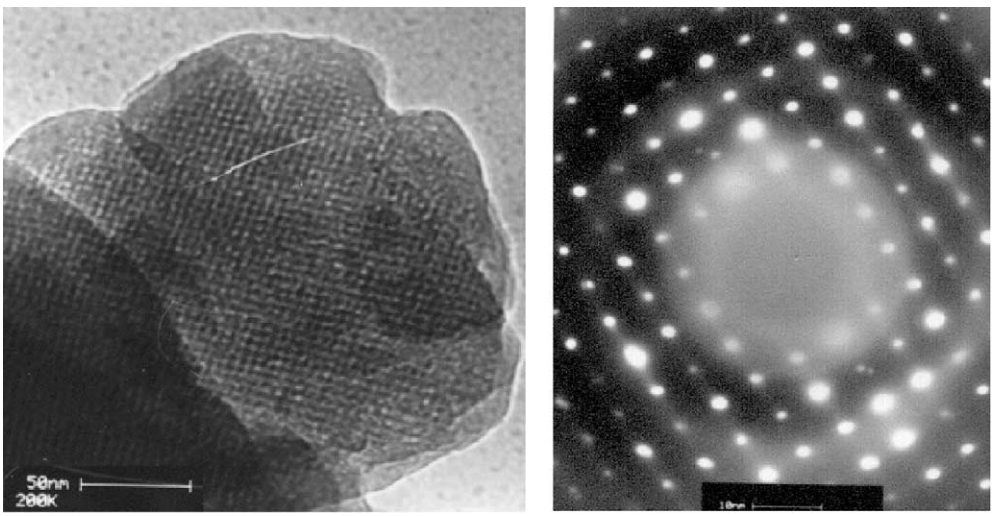

Fig. 3. TEM image and ED of calcined Na-AlMCM-48.

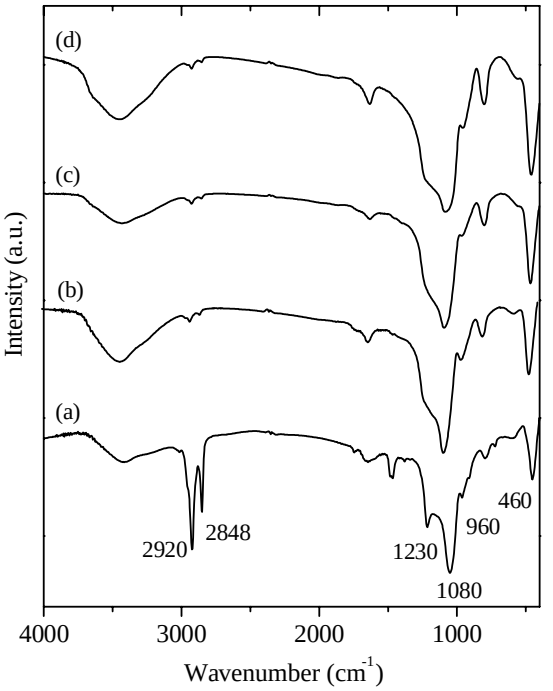

Fig. 4. FT-IR of: (a) as-synthesized Na-AlMCM-48, (b) calcined Na-AlMCM-48, (c) H-AlMCM-48 and (d) H-AlMCM-48 after reaction and calcined.

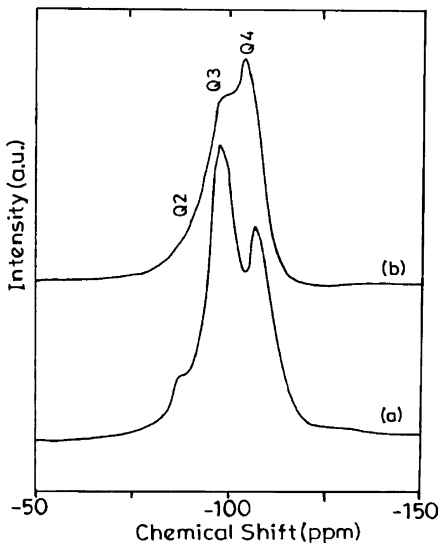

Fig. 5. ^{29}Si MAS-NMR spectra of Na-AlMCM-48: (a) as-synthesized and (b) calcined.

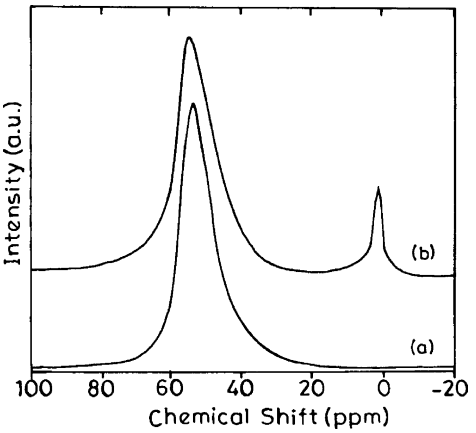

Fig. 6. ^{27}Al MAS-NMR of Na-AlMCM-48: (a) as-synthesized and (b) calcined.

$(Si(OSi)_2(OH)_2)$ [53]. Upon calcination, the Q_2 signal disappears and the intensity of Q_3 signal decreases indicating the condensation of silanol groups. Fig. 6 depicts the ^{27}Al MAS-NMR spectra of as-synthesized and calcined Na-AlMCM-48. The spectrum of the former shows a strong signal at 51.9 ppm corresponding to tetrahedral aluminum in the framework structure. However, upon calcination, the spectrum shows an additional weak signal around 0 ppm characteristic of aluminum in the octahedral coordination [28,29].

Fig. 7 depicts the NH_3-TPD profiles of H-AlMCM-48. The desorption peaks were deconvoluted using Gaussian function with temperature as variant [23]. The first peak, around 420–440 K, referred to

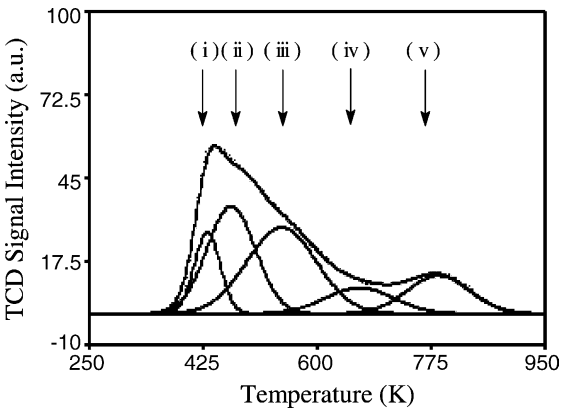

Fig. 7. NH_3-TPD profile of H-AlMCM-48.

as type (i), which is attributed to surface (defect) or terminal hydroxyl groups (weak Brönsted acid sites), whereas the two other peaks, viz. types (ii) and (iii), in the range 450–480 and 540–600 K hail from moderate and strong (Brönsted) acid sites. The latter two may originate owing the presence of trivalent aluminum in two different framework positions. The broad and weak peak around 650–700 K, designated as type (iv), is attributed to weak (structural) Lewis acid sites, which may arise from tri-coordinated aluminum in the framework. A further increase in temperature (820 K) resulted the appearance of another peak corresponding to strong Lewis acid sites originated from non-framework aluminum [29], which is in accordance with ^{27}Al MAS-NMR results (see Fig. 6b). Further, it can also be noticed from this figure that the area under the profiles corresponding to the moderate and strong Brönsted acid sites (i.e. types (ii) and (iii)) is much larger, which is in agreement with Pu et al. [15]. In addition, the relative amount of moderate-to-strong Brönsted acid sites is almost same as that of H-AlMCM-41 catalyst [23]. A schematic representation of the various acidic sites is shown in Scheme 2.

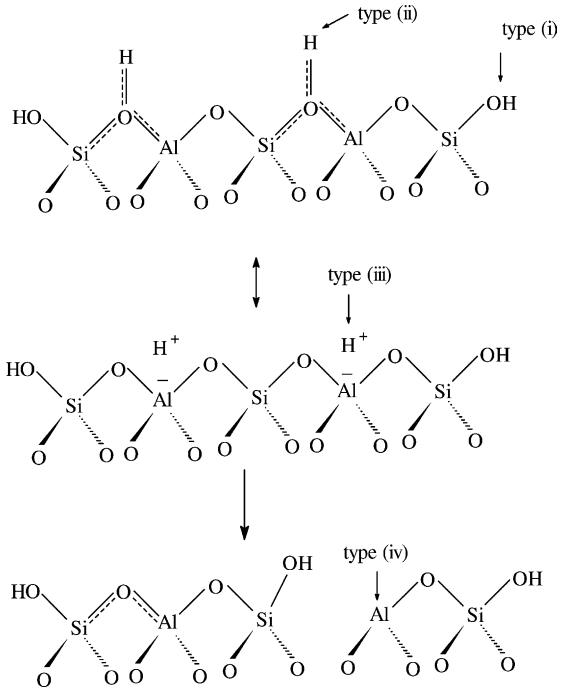

Scheme 2. Representation of different aluminum sites in AlMCM-41 and AlMCM-48.

Table 1
Comparison of H-AlMCM-48 and H-AlMCM-41 over *tertiary*-butylation of phenol

Reactant/products	H-AlMCM-48 [this work]	H-AlMCM-41 [23]
Phenol conversion (wt.%)	59.1	35.9
Selectivity (wt.%)		
o-*t*-BP	8.1	8.1
m-*t*-BP	2.5	4.7
p-*t*-BP	79.8	83.3
2,4-di-*t*-BP	9.6	3.9

Reaction conditions: $T = 448$ K; WHSV $= 4.8\,h^{-1}$; TOS $= 1.5$ h; *t*-BA:phenol = 2:1.

As can be seen from this scheme that the framework aluminum is responsible for the medium-to-strong Brönsted acid sites, which is useful for chosen reaction. On other hand, extra-framework/non-framework aluminum is responsible for Lewis acid sites and is not active for the reaction.

Table 1 presents the results of *tertiary*-butylation of phenol over H-AlMCM-48 under an optimized experimental condition. For comparison, the reaction results over H-AlMCM-41 are also included [23]. It can be seen from table that, the phenol activity is much higher in the case of H-AlMCM-48. However, it is noteworthy here that the distribution and amount of acid sites are almost same in both catalysts. Thus, the observed high activity of H-AlMCM-48 catalyst could be attributed to the three-dimensional pore opening, as against one-dimensional opening of H-AlMCM-41, which is entails more agitated flow in the system, and thereby increasing the number of interactions between reactants and catalytic sites [15]. On the other hand, the observed conversion of *t*-butanol is ∼95%. However, depending upon the reaction conditions and parameters, we do observe the oligomers, which are formed by the undesired reaction of C_4 hydrocarbons (formed from *t*-butanol) to produce C_8 and C_{12} fractions and is in agreement with literature reports [40,54].

The effect of time-on-stream (TOS) on phenol conversion over H-AlMCM-48 is shown in Fig. 8. For comparison, we have also included the effect of TOS on phenol conversion over H-AlMCM-41 (Fig. 9). It is clear from these figures that the H-AlMCM-48 catalyst does not get deactivated at higher phenol and/or t-BA content, which is in contrast to H-AlMCM-41 where

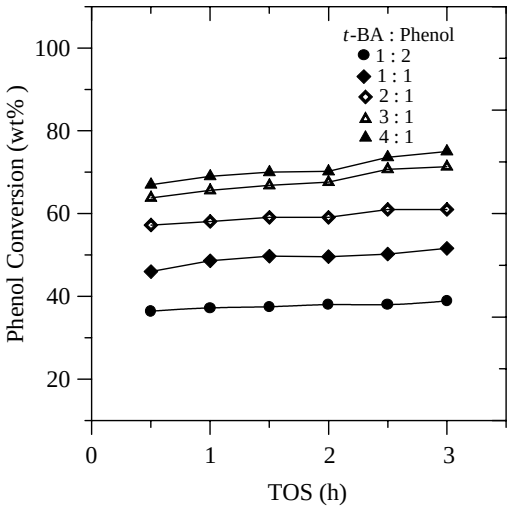

Fig. 8. Effect of TOS on the phenol conversion over H-AlMCM-48 (reaction conditions: $T = 448\,K$; WHSV $= 4.8\,h^{-1}$; *t*-BA: phenol = 2:1).

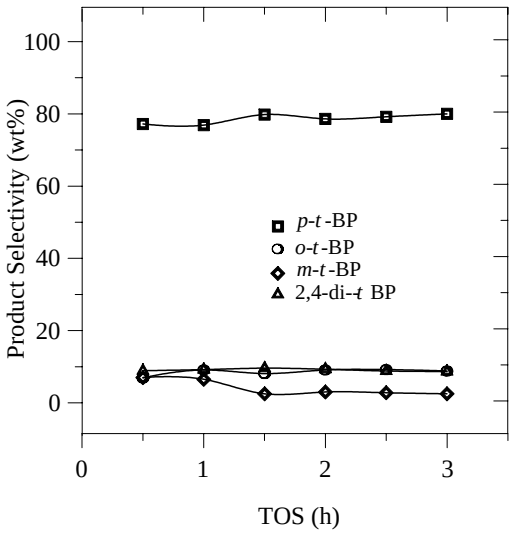

Fig. 10. Effect of TOS on the product selectivity over H-AlMCM-48 (reaction conditions: $T = 448\,K$; WHSV $= 4.8\,h^{-1}$; *t*-BA:phenol = 2:1).

the deactivation is clearly noticed [23]. The observed difference in the deactivation pattern could, however, be accounted to the three-dimensional pore system of the former as it is known to be more effective than the one-dimensional pore systems. The effect of TOS on product selectivity over H-AlMCM-48 is shown in Fig. 10. It can be seen from the figure that there is no considerable change in selectivity of the product, which was noticed after 1 h. Fig. 11 depicts the influence of temperature on the *tertiary*-butylation reaction over H-AlMCM-48 catalyst. It can be seen from this figure that the phenol conversion decreases as the reaction temperature increases, which could be due to a

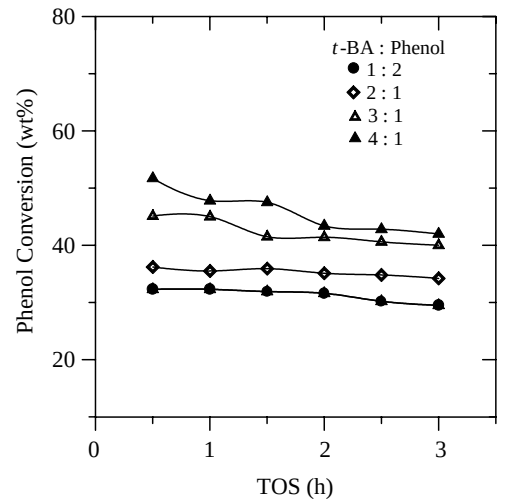

Fig. 9. Effect of TOS on the phenol conversion over H-AlMCM-41 (reaction conditions: $T = 448\,K$; WHSV $= 4.8\,h^{-1}$; *t*-BA: phenol = 2:1).

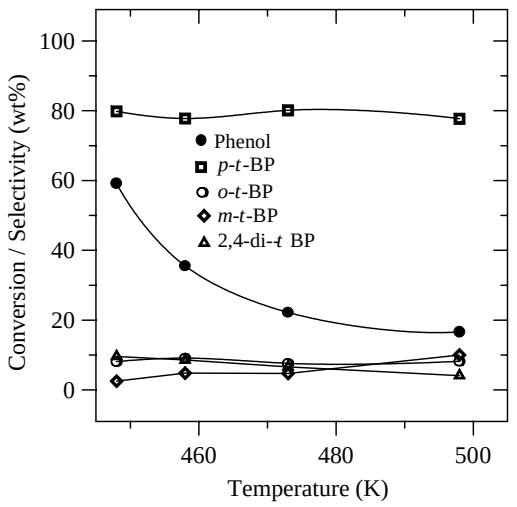

Fig. 11. Effect of temperature on the reaction over H-AlMCM-48 (reaction conditions: WHSV $= 4.8\,h^{-1}$; TOS = 1.5 h; *t*-BA: phenol = 2:1).

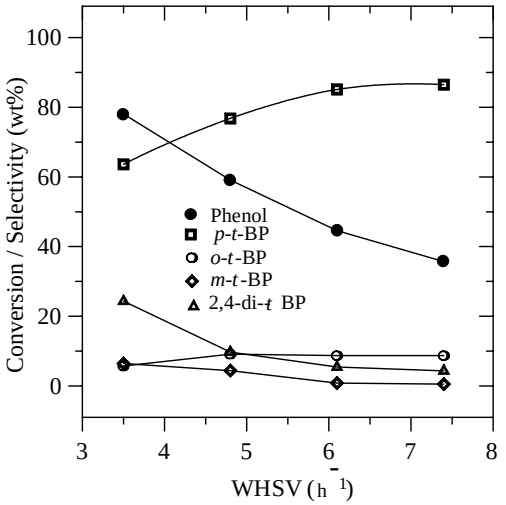

Fig. 12. Effect of WHSV on the reaction over H-AlMCM-48 (reaction conditions: $T = 448$ K; TOS = 1.5 h; *t*-BA:phenol = 2:1).

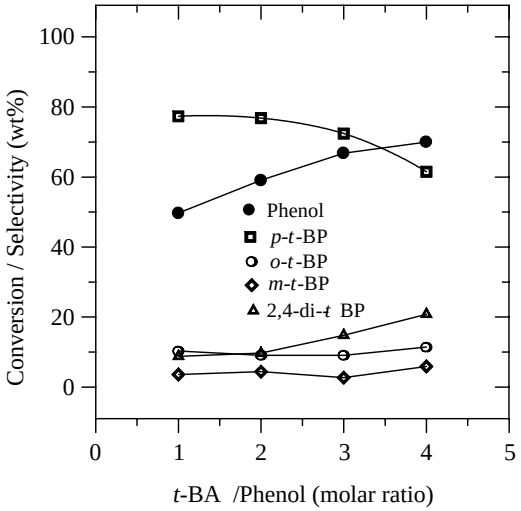

Fig. 13. Effect of *t*-BA-to-phenol molar ratio on the reaction over H-AlMCM-48 (reaction conditions: $T = 448$ K; WHSV = 4.8 h^{-1}; TOS = 1.5 h).

simultaneous dealkylation of *t*-BP leading to the formation of phenol [44] as well as oligomerization products [40,54]. Further, at higher temperature, 2,4-di-*t*-BP selectivity decreases owing to the absence of secondary alkylation, which again supports the dealkylation process at higher temperature. A similar trend was also observed in H-AlMCM-41 [23], H-GaMCM-41 [46], and HY and dealuminated HY [47].

Fig. 12 shows the effect of WHSV on reaction over H-AlMCM-48. It is clear from the figure that with the increase in WHSV, the substrate conversion monotonically decreases. However, the observed higher conversion at low WHSV could be due to more contact time of the reactant molecules as a consequence of the slow diffusion while the lower conversion at higher WHSV could be attributed to less contact time of the reactant molecules as a result of the faster diffusion. On other hand, the increase in mono-alkylated products could be attributed to the absence of secondary reaction as a consequence of less contact time of reactants/products with the catalyst. Fig. 13 presents the effect of *t*-BA-to-phenol (molar) ratio on the reaction over H-AlMCM-48. It can be seen from this figure that the phenol conversion increases with an increase in *t*-BA-to-phenol ratio. This is in good agreement with the general trend observed in literature [44], where the polar molecules such as methanol and higher alcohols compete with phenol for the adsorption sites, and with increasing molar excess of the alkylating agent, the phenol conversion increases. However, as can be noticed from Fig. 13 that an increase in *t*-BA content leads to a decrease in *p*-*t*-BP selectivity due to a possible secondary alkylation reaction resulting in the formation of 2,4-di-*t*-BP.

4. Conclusion

In summary, in this study, we presented the synthesis of high quality mesoporous Na-AlMCM-48 molecular sieves, and the samples were characterized systematically using various analytical and spectroscopic techniques. The H-AlMCM-48 catalyst was used for the acid catalyzed reaction, viz., *tertiary*-butylation of phenol. From the various studies, it was concluded that the mesoporous H-AlMCM-48 showed much higher activity. Unlike the analogous H-AlMCM-41, the H-AlMCM-48 catalyst does not get deactivated. Although, both these catalysts possess nearly the same amount of moderate-to-strong (Brönsted) acid sites, i.e. types (ii) and (iii), the H-AlMCM-48 catalyst exhibits increased activity that, however, could be attributed mainly to its three-dimensional pore structure. Thus, the mesoporous H-AlMCM-48 catalyst shows promise for the cho-

sen reaction and may well be suited for other acid catalyzed reactions.

Acknowledgements

The authors thank RSIC, IIT-Bombay for TEM, MAS-NMR and ICP-AES facilities, and Dr. A. Sakthivel and Mr. F. Hussain for the initial work as well as the experimental assistance.

References

[1] C.T. Kresge, M.E. Leonowicz, W.J. Roth, J.C. Vartuli, J.S. Beck, Nature 359 (1992) 710;
J.S. Beck, J.C. Vartuli, W.J. Roth, M.E. Leonowicz, K.D. Schmidtt, C.T.-W. Chu, D.H. Olson, E.W. Sheppard, S.B. McCullen, J.B. Higgins, J.L. Schlenker, J. Am. Chem. Soc. 114 (1992) 10834.
[2] A. Sayari, Chem. Mater. 8 (1996) 1840.
[3] A. Corma, Chem. Rev. 97 (1997) 2373.
[4] J.Y. Ying, C.P. Mehnert, M.S. Wong, Angew. Chem. Ind. Ed. 38 (1999) 56.
[5] D. Trong On, D. Desplantier-Giscard, C. Danumah, S. Kaliaguine, Appl. Catal. A 222 (2001) 299.
[6] P. Selvam, S.K. Bhatia, C. Sonwane, Ind. Eng. Chem. Res. 40 (2001) 3237.
[7] H. Kosslick, H. Landmesser, R. Fricke, J. Chem. Soc., Faraday Trans. 93 (1997) 1849.
[8] E. Armengol, M.L. Cano, A. Corma, F. Rey, J.L. Jorda, J. Chem. Soc., Chem. Commun. (1995) 519;
A. Corma, A. Martinez, V. Martinez-Soria, J.B. Monten, J. Catal. 153 (1995) 25.
[9] R. Mokaya, R.W. Jones, Z. Luan, M.D. Alba, J. Klinowski, Catal. Lett. 37 (1996) 113.
[10] X.S. Zhao, G.Q. Lu, G.J. Millar, Catal. Lett. 38 (1996) 33.
[11] B. Chakraborty, A.C. Pulikottil, B. Viswanathan, Catal. Lett. 39 (1996) 63.
[12] K.M. Reddy, C. Song, Catal. Today 31 (1996) 137.
[13] E.A. Gunnewegh, S.S. Gopie, H. van Bekkum, J. Mol. Catal. A 106 (1996) 151.
[14] J.H. Kim, M. Tanabe, M. Niwa, Microporous Mater. 10 (1997) 85.
[15] S.B. Pu, J.B. Kim, M. Seno, M.T. Inui, Microporous Mater. 10 (1997) 25.
[16] E. Armengol, A. Corma, H. Garcia, J. Primo, Appl. Catal. A 149 (1997) 411;
M.J. Climent, A. Corma, R. Guil-López, S. Iborra, J. Primo, J. Catal. 175 (1998) 70.
[17] J. Wang, L. Huang, H. Chen, Q. Li, Catal. Lett. 55 (1998) 157.
[18] R. Anwander, C. Palm, G. Gerstherger, O. Groeger, G. Engelhardt, Chem. Commun. (1998) 1811.
[19] I. Rodriguez, S. Iborra, A. Corma, F. Rey, J.L. Jorda, Chem. Commun. (1998) 593.
[20] C. Perego, S. Amarilli, A. Carati, C. Flego, G. Pazzuconi, C. Rizzo, G. Bellussi, Microporous Mesoporous Mater. 27 (1999) 345.
[21] J.P.G. Pater, P.A. Jacobs, J. Martens, J. Catal. 184 (1999) 262.
[22] K. Chaudhari, T.K. Das, A.J. Chandwadkar, S. Sivasanker, J. Catal. 186 (1999) 81.
[23] A. Sakthivel, S.K. Badamali, P. Selvam, Microporous Mesoporous Mater. 39 (2000) 457.
[24] S. Jun, R. Ryoo, J. Catal. 195 (2000) 237.
[25] K.G. Bhattacharyya, A.K. Talukdar, P. Das, S. Sivasanker, Catal. Commun. 2 (2001) 105.
[26] R. Schmidt, H. Junggreen, M. Stocker, Chem. Commun. (1996) 875.
[27] M. Hartmann, C. Bischof, Stud. Surf. Sci. Catal. 117 (1998) 249.
[28] A.A. Romero, M.D. Alba, J. Klinowski, J. Phys. Chem. B 102 (1998) 123.
[29] H. Kosslick, G. Lischke, H. Landmesser, B. Parlitz, W. Storek, R. Fricke, J. Catal. 176 (1998) 102;
H. Landmesser, H. Kosslick, U. Kurschner, R. Fricke, J. Chem. Soc., Faraday Trans. 94 (1998) 971.
[30] X. Auvray, C. Petipas, R. Anthore, I. Rico, A. Lattes, J. Phys. Chem. 93 (1989) 7458.
[31] W. Zhao, Y. Luo, P. Deng, Q. Li, Catal. Lett. 73 (2001) 199.
[32] A. Sakthivel, S.E. Dapurkar, P. Selvam, Catal. Lett. 77 (2001) 155.
[33] K. Vidya, S.E. Dapurkar, P. Selvam, S.K. Badamali, D. Kumar, N.M. Gupta, J. Mol. Catal. A 181 (2002) 91;
K. Vidya, S.E. Dapurkar, P. Selvam, S.K. Badamali, D. Kumar, N.M. Gupta, J. Mol. Catal. A 191 (2003) 149.
[34] A. Sakthivel, S.E. Dapurkar, P. Selvam, Appl. Catal. A 246 (2003) 283.
[35] E.H. Knozinger, J. Weitkamp, Handbook of Heterogeneous Catalysis, vol. 5, VCH, Weinheim, 1997;
J.H. Clark, D.J. Macquarrie, Org. Process Res. Dev. 1 (1997) 149.
[36] A.J. Kolka, J.P. Napolitano, G.G. Elike, J. Org. Chem. 21 (1956) 712.
[37] R.F. Parton, J.M. Jacobs, D.R. Huybrechts, P.A. Jacobs, Stud. Surf. Sci. Catal. 46 (1988) 163.
[38] C.V. Satyanarayana, U. Sridevi, B.S. Rao, Stud. Surf. Sci. Catal. 135 (2001) 238.
[39] A. Corma, H. Garcia, J. Primo, J. Chem. Res.(s) (1988) 40.
[40] K. Zhang, C. Huang, H. Zhang, S. Xiang, S. Liu, D. Xu, H. Li, Appl. Catal. A 166 (1998) 89.
[41] A. Mitra, Ph.D. Thesis, I.I.T.-Bombay, 1997.
[42] S. Namba, T. Yahima, Y. Itaba, H. Hara, Stud. Surf. Sci. Catal. 5 (1980) 105.
[43] C.D. Chang, S.D. Hellring, US Patent 5,288,927 (1994).
[44] S. Subramanian, A. Mitra, C.V.V. Satyanarayana, D.K. Chakrabarty, Appl. Catal. A 229 (1997) 159.
[45] S.K. Badamali, A. Sakthivel, P. Selvam, Catal. Lett. 65 (2000) 153.
[46] A. Sakthivel, P. Selvam, Catal. Lett. 84 (2002) 37.
[47] R. Anand, R. Maheswari, K.U. Gore, B.B. Tope, J. Mol. Catal. A 193 (2003) 251.

[48] A.V. Krishnan, K. Ojha, N.C. Pradhan, Org. Proc. Res. Dev. 6 (2002) 132.
[49] S.E. Dapurkar, S.K. Badamali, P. Selvam, Catal. Today 68 (2001) 63.
[50] R.D. Shannon, C.T. Prewitt, Acta Crystallogr. B 25 (1969) 925.
[51] R. Schmidt, M. Stöcker, M.D. Akporiaye, E.H. Tørstad, A. Olsen, Microporous Mater. 5 (1995) 1.
[52] A. Carlsson, M. Kaneda, Y. Sakamoto, O. Terasaki, R. Ryoo, S.H. Joo, J. Electron Microsc. 48 (1999) 795.
[53] C.Y. Chen, H-X. Li, M.E. Davis, Microporous Mater. 2 (1993) 17.
[54] Z. Liu, P. Moreau, F. Fajula, Appl. Catal. A 159 (1997) 305.